



New lignans, sesquiterpenes and other constituents from twigs and leaves of *Rhododendron micranthum*



Zhaoxin Zhang¹, Huimin Yan¹, Yuxun Zhu, Huanping Zhang, Lisha Chai, Li Li, Xiaojing Wang, Yunbao Liu, Yong Li^{*}

State Key Laboratory of Bioactive Substance and Function of Natural Medicines, Institute of Materia Medica, Chinese Academy of Medical Sciences & Peking Union Medical College, Beijing 100050, People's Republic of China

ARTICLE INFO

Keywords:

Rhododendron micranthum
Neolignans
Anti-inflammatory
NF- κ B

ABSTRACT

Rhododendron micranthum is used traditionally as a remedy for the treatment of chronic bronchitis in China. To clarify the chemical basis and provide a reference for the rational use of this medicinal plant, a phytochemical study was carried out on the twigs and leaves of *R. micranthum*, which afforded eight new compounds (1–8) and eight known compounds (9–16). Their structures were rigorously determined by comprehensive HRESIMS, NMR and electronic circular dichroism (ECD) analyses. The anti-inflammatory activities of these compounds were evaluated. Compounds 3, 13, and 14 suppressed the transcription of the NF- κ B-dependent reporter gene in LPS-induced 293T/NF- κ B-luc cells at 10 μ M, while no effect on cell viability was observed.

1. Introduction

Plants of *Rhododendron* are prolific sources of bioactive natural products, including flavonoids [1–3], lignans [4], diterpenoids [5–9], triterpenoids [10,11], sesquiterpenoids, and many other compounds. These compounds exhibit diverse significant activities, such as analgesic [8,12], antioxidant [3], and anti-inflammatory activities [13,14]. Among these plants, the twigs and leaves of *Rhododendron micranthum* (also known as zhaoshanbai) have been used as traditional Chinese medicine for various ailments, such as chronic bronchitis, sore swollen, menoxenia, postpartum arthralgia, and hypertension [15]. Among those diseases, chronic bronchitis, sore swollen, and postpartum arthralgia have a close relationship with inflammation. Presently, the extract of *R. micranthum* is still widely used in the treatment of chronic bronchitis in China. However, understanding of the chemical basis of its anti-inflammatory effects is still vague in general. Focusing on the discovery of new anti-inflammatory compounds and revealing the chemical basis of traditional Chinese medicine, a chemical study was carried out on the EtOH extract of the twigs and leaves of *R. micranthum*. Sixteen compounds, including eleven lignans (1–5, 9–11, 14–16), one phenolic glycoside (6), two sesquiterpenes (7–8), and two coumarins (12–13), were obtained. The structures of the new compounds were shown in Fig. 1. Several compounds, such as compounds 3, 13, and 14, showed moderate anti-inflammatory activities in an NF-

κ B reporter gene assay. Herein, the details of the isolation, structural identification, and bioactivity evaluation are presented.

2. Experimental section

2.1. General experimental procedures

IR spectra and UV were performed on a Nicolet 5700 FT-IR spectrometer and a JASCO V650 spectrometer. Optical rotations were obtained on a Rudolph automatic polarimeter. HRESI-MS data were acquired via an Agilent 6520 Accurate-Mass Q-TOF LC/MS spectrometer. ECD spectra were conducted on a circular dispersion spectrometer (JASCO J-815). NMR spectra were obtained on Bruker AV600-III, INOVA SX-600 and INOVA-500 spectrometer. Preparative HPLC was conducted on a Shimadzu LC-6AD instrument equipped with SPD-20A and RID-10A detectors (Kyoto, Japan) using a YMC Pack ODS-A column (250 \times 10 mm, 5 μ m, Kyoto, Japan). Macroporous resin (D101 type, The Chemical Plant of Nankai University, China), Sephadex LH-20 (GE Chemical Corporation, USA), silica gel and GF₂₅₄ TLC plates (Qingdao Marine Chemical Factory, China) and ODS (50 μ m, Merck, Germany) were used for column chromatography (CC). Spots were detected under UV light or spraying with 10% H₂SO₄ in EtOH-H₂O (95:5, v/v) followed by heating.

^{*} Corresponding author.

E-mail address: liyong@imm.ac.cn (Y. Li).

¹ Z.-X. Zhang and H.-M. Yan contributed equally.

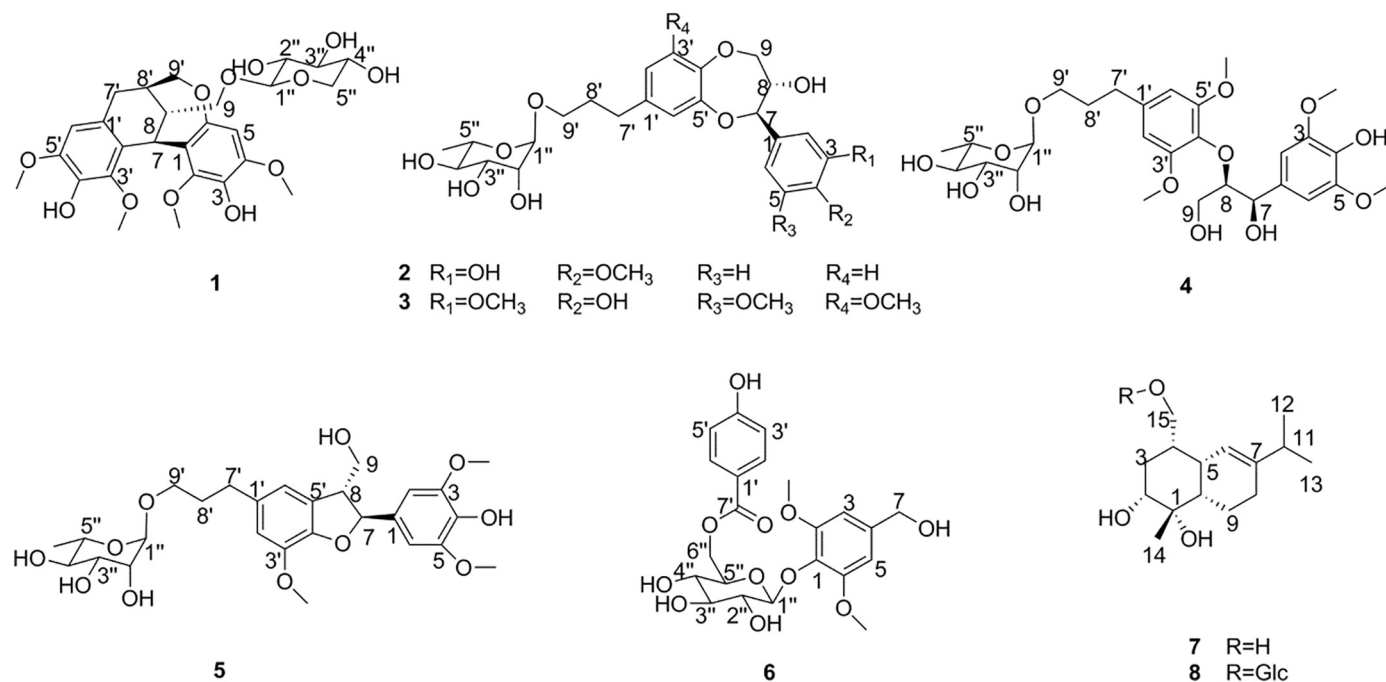


Fig. 1. Structures of compounds 1–8 isolated from the twigs and leaves of *R. micranthum*.

2.2. Plant material

The twigs and leaves of *R. micranthum* were collected in August 2014 from Shandong Province, China, and were authenticated by Prof. Peng Wan (Shandong Traditional Chinese Medicine University). A voucher specimen (ID-S-2586) was deposited in the herbarium at the Department of Medicinal Plants, Institute of Materia Medica, Chinese Academy of Medical Sciences.

2.3. Extraction and isolation

The dried twigs and leaves of *R. micranthum* (107.5 kg) were ground and extracted in EtOH-H₂O (95:5, v/v) twice (2 h each time) under reflux. The extract residue (12 kg) was suspended in H₂O (12L) and then partitioned sequentially with petroleum ether, CH₂Cl₂, EtOAc, and n-butanol. The EtOAc portion (2.7 kg) was then separated using macroporous resin CC and eluted with a mixture of EtOH-H₂O (30:70, 60:40, 95:5, v/v).

The 30% EtOH fraction (1.1 kg) was separated using silica gel CC, which was eluted with a mixture of CH₂Cl₂:MeOH (100:1–1:1, v/v) to obtain 9 fractions (E₃₀G₁–E₃₀G₉). Then, E₃₀G₄ (31 g) was separated using silica gel CC and eluted with a mixture of CH₂Cl₂:MeOH (100:1–1:1, v/v) to obtain 10 fractions (E₃₀G₄g₁–E₃₀G₄g₁₀). E₃₀G₄g₉ (3 g) was separated via Sephadex LH-20 CC, preparative HPLC and semipreparative HPLC, with MeCN-H₂O (19:81, v/v), to yield **1** (30.6 mg, t_R = 28.9 min). E₃₀G₃ (60 g) was purified on a Sephadex LH-20 CC to obtain 3 fractions (E₃₀G₃L₁–E₃₀G₃L₃). Next, E₃₀G₃L₁ was further purified by MCI CC to yield 6 fractions (E₃₀G₃L₁M₁–E₃₀G₃L₁M₆). Subsequently, E₃₀G₃L₁M₅ was dissolved with MeOH and filtered, and the solid was determined to be **12** (333.7 mg). The mother solution was separated via preparative HPLC and semipreparative HPLC with MeCN-H₂O (19:81, v/v) to yield **4** (2.3 mg, t_R = 37.3 min) and with MeCN-H₂O (21:79, v/v) to yield **9** (2.3 mg, t_R = 26.8 min). E₃₀G₅ (306.6 g) was further separated using Sephadex LH-20 CC to obtain 2 fractions (E₃₀G₅L₁–E₃₀G₅L₂). E₃₀G₅L₁ (37.7 g) was then separated via MCI CC and eluted with a step gradient of MeOH/H₂O (10:90, 30:70, 50:50, 60:40, 70:30 and 100:0, v/v) to yield 5 fractions (E₃₀G₅L₁M₁–E₃₀G₅L₁M₅). E₃₀G₅L₁M₂ was purified by preparative HPLC and semipreparative HPLC, with MeOH-H₂O (38:62, v/v) to yield **6** (26.3 mg,

t_R = 25.5 min); with MeCN-H₂O (14:86, v/v) to yield **13** (8.8 mg, t_R = 28.0 min); and with MeCN-H₂O (13:87, v/v) to yield **16** (70.0 mg, t_R = 79.1 min). E₃₀G₅L₁M₃ (11.9 g) was separated using ODS CC and eluted with a step gradient of MeOH/H₂O (10:90, 30:70, 50:50, 60:40, 70:30 and 100:0, v/v) to yield 5 fractions (E₃₀G₅L₁M₃O₁–E₃₀G₅L₁M₃O₅). Then, E₃₀G₅L₁M₃O₃ (4.3 g) was purified by preparative HPLC and semipreparative HPLC with MeCN-H₂O (15:85, v/v) to yield **15** (44.0 mg, t_R = 12.2 min). E₃₀G₅L₁M₄ was separated with MeCN-H₂O (25:75, v/v) to yield **2** (8.0 mg, t_R = 41.2 min); with MeCN-H₂O (20:80, v/v) to yield **5** (2.2 mg, t_R = 46.5 min), **3** (7.5 mg, t_R = 57.6 min) and **10** (14.3 mg, t_R = 46.3 min); and with MeCN-H₂O (21:79, v/v) to yield **11** (3.9 mg, t_R = 26.0 min). E₃₀G₅L₁M₅ was purified with MeCN-H₂O (14:86, v/v) to yield **14** (36.0 mg, t_R = 41.9 min).

The 60% EtOH fraction (288 g) was separated using silica gel CC and eluted with a mixture of CH₂Cl₂:MeOH (100:1–1:1, v/v) to obtain 9 fractions (E₆₀G₁–E₆₀G₉). E₆₀G₂, E₆₀G₃, E₆₀G₆, and E₆₀G₈ were then all separated via Sephadex LH-20 CC. Fraction E₆₀G₃ was separated by Sephadex LH-20 CC and eluted with MeOH–H₂O (60:40, v/v), yielding three fractions (E₆₀G₃L₁–E₆₀G₃L₃). E₆₀G₃L₂ was purified by preparative HPLC and semipreparative HPLC with MeCN-H₂O (25:75, v/v) to yield **7** (8.4 mg, t_R = 67.9 min). E₆₀G₈L₂ was purified by preparative HPLC and semipreparative HPLC with MeCN-H₂O (20:80, v/v) to yield **8** (6.9 mg, t_R = 31.2 min).

Rhodomicanthoside A (**1**): white powder; [α]_D²⁰ + 147.7 (c 0.56, MeOH); IR(KBr) ν_{max} 3419, 2937, 1675, 1615, 1498, 1459, 1354, 1310, 1239, 1196, 1122, 1089, 975, 943, 917, 890, 868, 835, 806, 624 cm⁻¹; for ¹H and ¹³C NMR spectroscopic data, see Tables 1 and 2; HRESI-MS(positive): m/z 573.1938 [M + Na]⁺ (calcd for C₂₇H₃₄NaO₁₂, 573.1942).

Rhodomicanthoside B (**2**): white powder; [α]_D²⁰ – 52.6 (c 0.29, MeOH); IR(KBr) ν_{max} 3389, 2921, 1676, 1615, 1505, 1458, 1368, 1276, 1240, 1202, 1126, 1047, 982, 944, 913, 863, 807, 721, 646 cm⁻¹; for ¹H and ¹³C NMR spectroscopic data, see Tables 1 and 2; HRESI-MS (positive): m/z 515.1889 [M + Na]⁺ (calcd for C₂₅H₃₂NaO₁₀, 515.1888).

Rhodomicanthoside C (**3**): white powder; [α]_D²⁰ – 22.8 (c 0.40, MeOH); IR(KBr) ν_{max} 3370, 2933, 1678, 1616, 1597, 1510, 1455, 1431, 1339, 1206, 1120, 1048, 982, 910, 880, 835, 742, 723, 655 cm⁻¹; for ¹H and ¹³C NMR spectroscopic data, see Tables 1 and 2; HRESI-MS

Table 1
¹H NMR spectroscopic data for compounds 1–6 in pyridine-d₅ (δ_H in ppm, J in Hz).

No.	1 ^a	2 ^b	3 ^b	4 ^a	5 ^a	6 ^b
2	–	7.38 s	7.17 s	7.24 d (2.8)	7.13 d (1.5)	–
3	–	–	–	–	–	6.98 s
5	6.52 s	7.30 s	–	–	–	6.98 s
6	–	7.30 s	7.17 s	7.24 d (2.8)	7.13 d (1.5)	–
7	5.17 s	5.43 dd (2.7, 8.1)	5.51 d (8.1)	5.76 br s	6.10 d (7.2)	4.95 s
8	2.71 t (7.3)	4.37 m	4.36 m	4.89 m	4.06 m	–
9	(b) 4.44 dd (7.1, 9.5) (a) 3.82 m	4.17 dd (2.5, 12.5) 3.91 m	4.26 m 3.93 m	4.66 ddd (2.4, 5.3, 11.9) 4.25 m	4.34 m 4.31 m	–
2'	–	6.81 dd (2.2, 8.3)	6.63 d (2.0)	6.65 d (2.9)	6.89 s	8.14 d (8.7)
3'	–	7.10 d (8.3)	–	–	–	7.16 d (8.7)
4'	–	–	–	–	–	–
5'	–	–	–	–	–	7.16 d (8.7)
6'	6.60 s	7.05 d (2.2)	6.79 d (2.0)	6.65 d (2.9)	7.04 s	8.14 d (8.7)
7'	(b) 3.35 dd (7.3, 17.3) (a) 3.04 d (17.2)	2.68 m	2.73 m	2.73 m	2.73 m	–
8'	2.55 dd (1.2, 7.4)	1.97 m	2.02 m	1.98 m	1.98 m	–
9'	4.52 dd (3.0, 12.0) 3.92 d (12.0)	3.89 m 3.53 dt (6.1, 9.5)	3.96 m 3.56 dt (6.1, 9.5)	3.92 m 3.54 m	3.93 m 3.54 m	–
1''	4.78 d (7.5)	5.27 br s	5.29 br s	5.29 br s	5.29 br s	5.76 d (7.6)
2''	4.08 dd (7.4, 8.9)	4.57 m	4.59 dd (1.7, 3.4)	4.58 m	4.60 dt (1.6, 3.3)	4.43 dd (7.6, 8.9)
3''	4.19 t (8.7)	4.52 m	4.53 dd (3.4, 9.1)	4.52 m	4.54 dd (3.5, 9.2)	4.37 t (8.8)
4''	4.25 ddd (5.2, 8.4, 10.1)	4.29 br t (9.5)	4.30 t (9.2)	4.30 td (2.2, 9.2)	4.30 m	4.28 t (9.8)
5''	4.33 dd (5.2, 11.3) 3.71 d (11.3)	4.22 m	4.22 m	4.21 m	4.23 m	4.13 ddd (2.2, 6.1, 9.8)
6''	–	1.66 dd (3.2, 6.1)	1.66 d (6.1)	1.66 dd (2.7, 6.1)	1.66 d (6.1)	5.14 dd (2.2, 11.7) 4.90 dd (6.1, 11.7) 3.73 s
2-OCH ₃	3.86 s	–	–	–	–	–
3-OCH ₃	–	–	3.81 s	3.77 d (2.8)	3.71 d (1.5)	–
4-OCH ₃	3.64 s	3.77 d (2.7)	–	–	–	–
5-OCH ₃	–	–	3.81 s	3.77 d (2.8)	3.71 d (1.5)	–
6-OCH ₃	–	–	–	–	–	3.73 s
3'-OCH ₃	4.14 s	–	3.86 s	3.79 d (2.8)	3.87 d (1.5)	–
5'-OCH ₃	3.69 s	–	–	3.79 d (2.8)	–	–

^a Recorded at 600 MHz.

^b Recorded at 500 MHz.

(positive): *m/z* 575.2104 [M + Na]⁺ (calcd for C₂₇H₃₆NaO₁₂, 575.2099).

Rhodomicroanthoside D (4): white powder; [α]_D²⁰ – 44.8 (c 0.36, MeOH); IR(KBr) ν_{max} 3393, 2921, 2850, 1677, 1646, 1508, 1464, 1424, 1327, 1276, 1207, 1126, 1050, 983, 911, 808, 721, 647 cm⁻¹; for ¹H and ¹³C NMR spectroscopic data, see Tables 1 and 2; HRESI-MS (positive): *m/z* 584.2493 [M + Na]⁺ (calcd for C₂₈H₄₀NaO₁₃, 584.2469).

Rhodomicroanthoside E (5): white powder; [α]_D²⁰ – 21.5 (c 0.33, MeOH); IR(KBr) ν_{max} 3387, 2921, 2850, 1678, 1646, 1615, 1518, 1501, 1464, 1427, 1326, 1272, 1207, 1124, 1050, 983, 952, 911, 837, 807, 721, 645 cm⁻¹; for ¹H and ¹³C NMR spectroscopic data, see Tables 1 and 2; HRESI-MS (positive): *m/z* 559.216 [M + Na]⁺ (calcd for C₂₇H₃₆NaO₁₁, 559.215).

Rhodomicroanthoside F (6): white powder; [α]_D²⁰ – 63.6 (c 0.33, MeOH); IR(KBr) ν_{max} 3431, 3228, 2962, 2928, 1692, 1598, 1508, 1460, 1425, 1377, 1361, 1330, 1314, 1281, 1240, 1167, 1125, 1080, 1040, 1017, 962, 903, 879, 850, 831, 816, 769, 693, 621, 601, 531 cm⁻¹; for ¹H and ¹³C NMR spectroscopic data, see Tables 1 and 2; HRESI-MS (positive): *m/z* 489.1379 [M + Na]⁺ (calcd for C₂₂H₂₆NaO₁₁, 489.1367).

Rhodomicroanthin I (7): yellow oil; [α]_D²⁰ – 9.0 (c 1.23, MeOH); IR(KBr) ν_{max} 3388, 2933, 2874, 1706, 1460, 1379, 1073, 1041, 623 cm⁻¹; for ¹H and ¹³C NMR spectroscopic data, see Table 3; HRESI-MS (positive): *m/z* 277.1772 [M + Na]⁺ (calcd for C₁₅H₂₆NaO₃, 277.1774).

Rhodomicroanthoside G (8): white powder; [α]_D²⁰ – 25.4 (c 0.59, MeOH); IR(KBr) ν_{max} 3382, 2923, 1676, 1426, 1379, 1202, 1136, 1079, 1043, 898, 839, 801, 722, 630 cm⁻¹; for ¹H and ¹³C NMR spectroscopic data, see Table 3; HRESI-MS (positive): *m/z* 439.2298 [M + Na]⁺ (calcd for C₂₁H₃₆NaO₈, 439.2302).

2.4. Determination of absolute configuration of sugar moieties

Each compound (1.5 mg) was added to 2 N HCl (2 mL) and refluxed for 12 h at 90 °C. The solution was extracted three times with EtOAc. The water layer was dried to yield a residue. Then, the residue was dissolved in pyridine (1 mL), and L-cysteine methyl hydrochloride (2 mg) was added. The mixture was refluxed for 2 h at 60 °C, dried by nitrogen and heated for 0.5 h at 80 °C. Next, *N*-trimethylsilylimidazole (1 mL) was added, and the mixture was heated for 2 h at 60 °C. Finally, the mixture was added to H₂O (2 mL) and partitioned with *n*-hexane (2 mL) three times. The organic layer was combined and concentrated and used for GC analysis. Preparation of the other compounds was conducted in the same way. The conditions of the GC experiments were as follows: capillary CC, HP-5 (60 m × 0.25 mm, with a 0.25 μm film, Dikma); detector, FID; injector temperature, 300 °C; detector temperature, 300 °C; initial temperature, 200 °C, increased to 280 °C at the rate of 10 °C/min, sustained for 35 mins, decreased to 200 °C at the rate of 40 °C/min and then sustained for 1 min; carrier gas, N₂. In the GC chromatogram, the retention times of the derivatives of standard D-glucose, D-xylose, and L-rhamnose were 29.6 min, 20.9 min and 23.5 min, respectively.

2.5. NF-κB reporter gene assay

For the cytotoxicity assay, the cytotoxicity of compounds on 293T cells was determined via an MTT assay. 293T cells were placed in 96-well plates (5 × 10³/well) overnight. The cells were then treated with 10 μM of compounds for 24 h. An equal concentration of the solvent vehicle (DMSO, 0.5%) was included as a control. Subsequently, 20 μL of MTT (5 mg/mL in sterile PBS) was added to each well for an additional 4 h incubation period. Finally, the medium was removed,

Table 2
¹³C NMR spectroscopic data for compounds 1–6 in pyridine-d₅ (δ_C in ppm).

No.	1 ^a	2 ^b	3 ^b	4 ^a	5 ^a	6 ^b
1	125.7, C	129.2, C	128.2, C	133.9, C	130.8, C	135.0, C
2	148.3, C	112.5, CH	106.6, CH	105.9, CH	105.3, CH	154.5, C
3	137.6, C	149.3, C	149.7, C	149.4, C	149.8, C	105.5, CH
4	147.9, C	149.2, C	138.6, C	137.1, C	138.1, C	140.3, C
5	102.6, CH	117.0, CH	149.7, C	149.4, C	149.8, C	105.5, CH
6	153.6, C	122.0, CH	106.6, CH	105.9, CH	105.3, CH	154.5, C
7	31.9, CH	77.6, CH	77.8, CH	74.3, CH	89.2, CH	64.8, CH ₂
8	42.6, CH	80.3, CH	80.2, CH	88.4, CH	55.6, CH	–
9	72.8, CH ₂	62.0, CH ₂	61.9, CH ₂	61.7, CH ₂	64.6, CH ₂	–
1'	126.9, C	135.6, C	134.8, C	138.7, C	135.6, C	122.2, C
2'	124.5, C	122.2, CH	106.0, CH	106.9, CH	113.9, CH	132.9, CH
3'	147.4, C	117.6, CH	150.0, C	154.3, C	145.2, C	116.5, CH
4'	139.3, C	143.2, C	133.0, C	135.3, C	147.9, C	163.9, C
5'	148.7, C	145.1, C	145.7, C	154.3, C	133.2, C	116.5, CH
6'	107.4, CH	117.9, CH	110.5, CH	106.9, CH	118.0, CH	132.9, CH
7'	30.1, CH ₂	32.5, CH ₂	33.0, CH ₂	33.5, CH ₂	33.1, CH ₂	167.0, C
8'	34.8, CH	32.3, CH ₂	32.3, CH ₂	32.2, CH ₂	32.7, CH ₂	–
9'	80.9, CH ₂	67.2, CH ₂	67.3, CH ₂	67.2, CH ₂	67.3, CH ₂	–
1''	106.3, CH	102.1, CH	102.2, CH	102.2, CH	102.2, CH	105.3, CH
2''	75.6, CH	72.8, CH	72.9, CH	72.8, CH	72.9, CH	76.5, CH
3''	79.1, CH	73.4, CH	73.4, CH	73.4, CH	73.4, CH	78.8, CH
4''	71.6, CH	74.5, CH	74.5, CH	74.4, CH	74.5, CH	72.2, CH
5''	67.7, CH ₂	70.3, CH	70.3, CH	70.3, CH	70.3, CH	76.2, CH
6''	–	19.1, CH ₃	19.1, CH ₃	19.1, CH ₃	19.1, CH ₃	65.1, CH ₂
2-OCH ₃	60.1, CH ₃	–	–	–	–	56.9, CH ₃
3-OCH ₃	–	–	56.8, CH ₃	56.8, CH ₃	56.8, CH ₃	–
4-OCH ₃	56.4, CH ₃	56.4, CH ₃	–	–	–	–
5-OCH ₃	–	–	56.8, CH ₃	56.8, CH ₃	56.8, CH ₃	–
6-OCH ₃	–	–	–	–	–	56.9, CH ₃
3'-OCH ₃	61.6, CH ₃	–	56.4, CH ₃	56.6, CH ₃	56.7, CH ₃	–
5'-OCH ₃	56.3, CH ₃	–	–	56.6, CH ₃	–	–

^a Recorded at 150 MHz.^b Recorded at 125 MHz.**Table 3**
¹H and ¹³C NMR data of compounds 7, 8 in pyridine-d₅ (δ_H and δ_C in ppm).

No.	7 ^a	7 ^b	8 ^a	8 ^b
1	–	74.9, C	–	74.9, C
2	4.63 m	73.9, CH	4.52 m	73.9, CH
3	2.28 m	39.8, CH ₂	2.15 m	39.2, CH ₂
	2.04 m	–	2.02 m	–
4	2.51 m	42.7, CH	2.58 m	40.1, CH
5	2.60 m	40.5, CH	2.50 m	40.2, CH
6	6.12 d (3.7)	124.6, CH	5.97 d (3.4)	124.3, CH
7	–	148.5, C	–	148.8, C
8	2.33 m	25.6, CH ₂	2.28 m	25.6, CH ₂
	2.00 m	–	1.96 m	–
9	1.95 m	43.8, CH ₂	1.91 m	43.7, CH ₂
	1.84 m	–	1.81 m	–
10	2.43 dd (7.3, 11.5)	62.2, CH	2.34 dd (7.6, 11.5)	61.3, CH
11	2.24 m	38.2, CH	2.21 m	38.2, CH
12	0.99 s	21.8, CH ₃	0.96 d (2.5)	21.8, CH ₃
13	1.00 s	22.1, CH ₃	0.98 d (2.5)	22.1, CH ₃
14	1.48 s	23.4, CH ₃	1.44 s	23.5, CH ₃
15	4.18 dd (5.6, 10.5)	64.3, CH ₂	4.54 m	72.2, CH ₂
	4.11 dd (6.0, 10.6)	–	3.91 m	–
1'	–	–	4.93 d (7.8)	105.6, CH
2'	–	–	4.07 m	75.8, CH
3'	–	–	4.26 m	79.1, CH
4'	–	–	4.24 m	72.3, CH
5'	–	–	3.97 m	79.0, CH
6'	–	–	4.57 m	63.4, CH ₂
	–	–	4.40 dd (5.4, 11.7)	–

^a Recorded at 500 MHz.^b Recorded at 125 MHz.

100 μL of DMSO was added to each well, and the absorbance (A) was detected at 490 nm using a microplate reader;

To determine the effect of compounds on the NF-κB signaling

pathway, a luciferase assay was performed to analyze the transcription of an NF-κB-dependent reporter gene as described previously. 293T/NF-κB-luc cells were seeded into 96-well plates at a density of 5 × 10⁵ per well. After 24 h incubation, cells were pretreated with compounds (10 μM) for 30 min before LPS (500 ng/mL) stimulation. An equal concentration of the solvent vehicle (DMSO, 0.5%) was always included as a control. After 6 h of stimulation, the medium was removed, and the cells were lysed with lysis buffer in the luciferase assay system. Afterward, the cell lysate was mixed with the luciferase assay reagent, and the luminescence of firefly luciferase was immediately quantified using a microplate reader.

3. Results and discussion

Compound 1 was obtained as a white powder, and the molecular formula was determined by analysis of the positive HRESIMS data (*m/z* 573.1938, calcd for C₂₇H₃₄NaO₁₂, 573.1942), indicating an index of hydrogen deficiency (IHD) of 11. The IR spectrum of this compound showed signals typical of hydroxy groups (3419 cm⁻¹) and aromatic rings (1615, 1498, 1459 cm⁻¹). The ¹H NMR data (Table 1) of 1 showed characteristic signals for four aromatic methoxy groups (δ_H 4.14, 3.86, 3.69 and 3.64), two aromatic protons (δ_H 6.60 and 6.52), and an anomeric proton (δ_H 4.78). The ¹³C NMR data (Table 2) displayed 27 carbon resonances, including four methyl groups, four methylenes, nine methines (two aromatic methines at δ_C 107.4 and 102.6 and an anomeric carbon of sugar at δ_C 106.3), and 10 quaternary carbons. The COSY and HSQC spectra showed the presence of the following fragments (Fig. 2): –CH(O)-CH(OH)-CH(OH)-CH(OH)-CH₂(O)-, –CH₂-CH-CH₂-, –CH-CH-CH₂-, and –CH-CH-. The HMBC correlation (Fig. 2) between H₂-9' and C-6, and the additional IHD suggested the presence of an oxygen bridge between C-9' and C-6. Additionally, the correlation between the anomeric proton (H-1'') and C-9 placed the

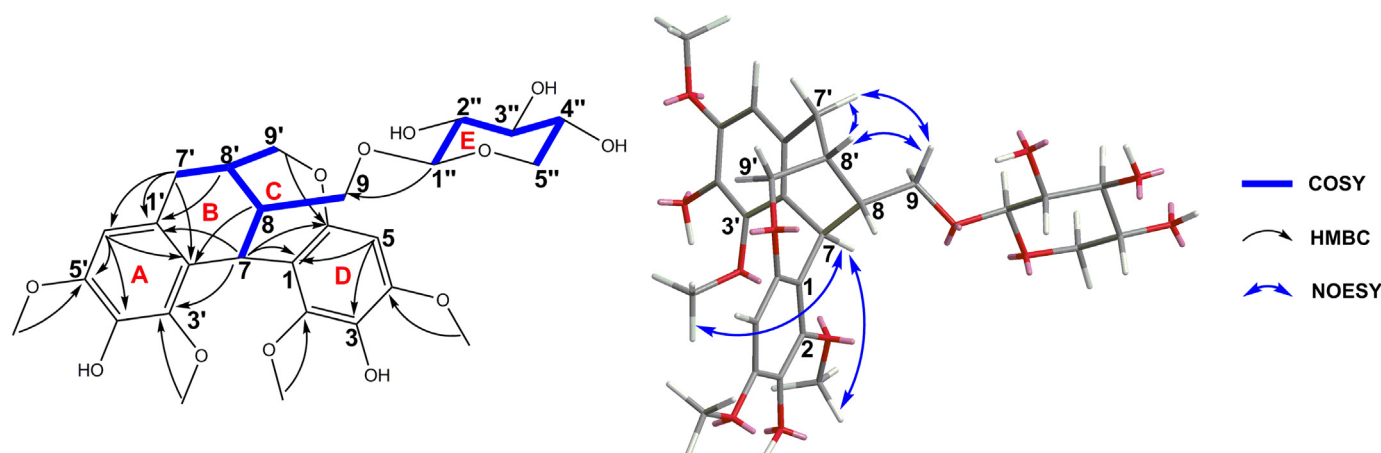


Fig. 2. ^1H – ^1H COSY (blue bold lines), key HMBC correlations (black arrows), and NOESY correlations (blue arrows) for compound 1. (For interpretation of the references to colour in this figure legend, the reader is referred to the web version of this article.)

pentose moiety at C-9. The pentose moiety was determined to be in a β -configuration due to the relatively large coupling constant of $J_{1'',2''}$ (7.5 Hz). Acid hydrolysis and GC analysis of **1** confirmed that the sugar moiety was *D*-xylose. The torsion angle between the two aromatic rings was approximately 90° . C-1 and C-9' were supposed to be on the same side of the six-membered ring (ring B in Fig. 2), which allowed the seven-membered ring to exist stably. Therefore, H-8' and H-7 should be on the other side of the ring (α -side). This assignment was confirmed by the NOE correlations between H-7/H-(2-OCH₃) and H-7/H-(3'-OCH₃). NOE correlations of H-7'b/H-9a, H-8'/H-7'b, and H-8'/H-9a indicated that H-7'b, CH₂-9, and H-8' were on the same side (α -side) of ring B while H-8 and H-7'a were on the other side (β -side). Accordingly, the relative configuration was determined. Contrary to (+)-ovafolinin B-9'-O- β -*D*-glucopyranoside [16], compound **1** showed a negative Cotton effect at 282 nm, which indicated the *7R* configuration of **1** [16–20]. Consequently, compound **1** was determined as (7*R*,8*R*,8'*R*)-ovafolinin B-9'-O- β -*D*-xylopyranoside and was given the trivial name rhomicranoside A.

Compound **2** was obtained as a white powder. The molecular formula was determined to be C₂₅H₃₂O₁₀ based on its pseudomolecular positive ion at m/z 515.1889 [M + Na]⁺ (calcd for 515.1888), indicating an IHD of 10. The ^1H and ^{13}C NMR data of **2** consist of the features of a lignan rhamnoside. The structure was determined by the HSQC, HMBC and CIGAR spectra. In the CIGAR spectrum, the correlations of H-7/C-5', H-8/C-1, and H-9/C-4' indicated the presence of a seven-membered ring, in which two C₆-C₃ moieties were connected via 5'-O-7 and 9-O-4' oxygen bridges. In addition, HMBC correlations of H-9'/C-1'' and H-1''/C-9' suggested that the rhamnose was connected to C-9'. Furthermore, the anomeric proton of the rhamnose showed a broad single peak at δ_{H} 5.27, which indicated that the rhamnose is in the α -configuration. The large coupling constant of $J_{7,8}$ (8.1 Hz), as well as the NOESY correlations of H-8/H-6 and H-8/H-2, indicated that H-7 and H-8 were in the *trans*-configuration. A positive Cotton effect at 231 nm was observed in the ECD spectrum, which suggested an *8S* configuration [21]. Additionally, acid hydrolysis and GC analysis of **2** confirmed that the sugar moiety was *L*-rhamnose. Thus, the structure of **2** was determined as (7*R*, 8*S*)-4-methoxy-5',7-epoxy-9,4'-epoxyneolignan-3,8-diol-9'-O- α -*L*-rhamnoside and was named rhomicranoside B.

Compound **3**, a white powder, was determined to have a molecular formula of C₂₇H₃₆O₁₂ based on its HRESI-MS peak at m/z 575.2104 [M + Na]⁺ (calcd for 575.2099). The NMR data of **3** were comparable to those of **2**, except for the substituents on benzene rings. According to the HSQC and HMBC data, in **3**, a hydroxy group instead of a methoxy group was located at C-4, and three hydroxy groups at C-3, C-3', and C-5 were all methylated. The large coupling constant of $J_{7,8}$ (8.1 Hz), as

well as the NOESY correlations of H-8/H-6 and H-8/H-2, indicated that H-7 and H-8 were in the *trans*-configuration. A positive Cotton effect at 238 nm in the ECD spectrum suggested the *S* configuration of C-8 [21]. Accordingly, compound **3** was determined to be (7*R*, 8*S*)-3,5,3'-trimethoxy-5',7-epoxy-9,4'-epoxyneolignan-4,8-diol-9'-O- α -*L*-rhamnoside and was named rhomicranoside C.

The HRESIMS data of **4** showed a pseudomolecular positive ion at m/z 584.2493 [M + Na]⁺ (calcd for 584.2469), indicating a molecular formula of C₂₈H₄₀O₁₃. The NMR data of **4** were similar to the data of (7*R*,8*R*)-4-hydroxy-9'-O-(α -*L*-rhamnopyranosyl)-3,3',5'-trimethoxy-8-O-4'-neolignan [22], except for an additional methoxy group. The HMBC correlations from H-(CH₃O-3/5) to C-3/5 placed the additional methoxy group at C-5. In the HMBC spectrum, the correlation of H-1'' and C-9' suggested that the rhamnose was attached at C-9'. Furthermore, the anomeric proton of the rhamnose at δ_{H} 5.29 (H-1'') was a broad single peak, indicating that the rhamnose was in the α -configuration. Meanwhile, H-7 (δ_{H} 5.76) showed a broad single peak, indicating that H-7 and H-8 were in the *erythro*-configuration [23]. Furthermore, a negative Cotton effect at 247 nm was observed in the ECD spectrum, which revealed the *8R* configuration [22,24]. Thus, compound **4** was determined as (7*R*, 8*R*)-4,7,9-trihydroxy-9'-O-(α -*L*-rhamnopyranosyl)-3,3',5,5'-tetramethoxy-8-O-4'-neolignan and was named rhomicranoside D.

Based on the HRESIMS peak at m/z 559.216 (calcd 559.215 [M + Na]⁺), the molecular formula of **5** was determined to be C₂₇H₃₆O₁₁. The NMR data showed that **5** was closely related to chaenomiside A [25]. However, HMBC correlations from H-1'' to C-9' and from H-9' to C-1'' indicated that the rhamnose was attached at C-9' in **5** instead of at C-9 in chaenomiside A. The broad single peak of the anomeric proton at δ_{H} 5.29 (H-1'') confirmed that the rhamnose was in the α -configuration. After acid hydrolysis of **5**, the absolute configuration of the rhamnose was determined by GC analyses. The C-7/C-8 relative configuration was assigned as the *trans*-form, according to the NOESY correlations of H₂-9/H-7 and H-8/H-2(6). The ECD spectrum showed two negative Cotton effects at 239 nm and 288 nm, which suggested the *7S* and *8R* configuration of **5** [26]. Finally, **5** was determined to have the structure (7*S*,8*R*)-3,5,3'-trimethoxy-4',7-epoxy-8,5'-neolignan-4,9-diol-9'-O- α -*L*-rhamnopyranoside and was named rhomicranoside E.

Compound **6**, a white powder, was determined to have a molecular formula of C₂₂H₂₆O₁₁ based on the HRESIMS data. The NMR data showed that **6** was closely related to saccharoside B [27]. The HMBC correlations from H-(CH₃O-2) to C-2 and those from H-(CH₃O-6) to C-6 revealed the location of the methoxy substitutions in **6**. The coupling constant of the anomeric proton ($J_{1'',2''} = 7.6$ Hz) suggested that glucose was in the β -configuration. Acid hydrolysis of **6** gave a β -*D*-glucose,

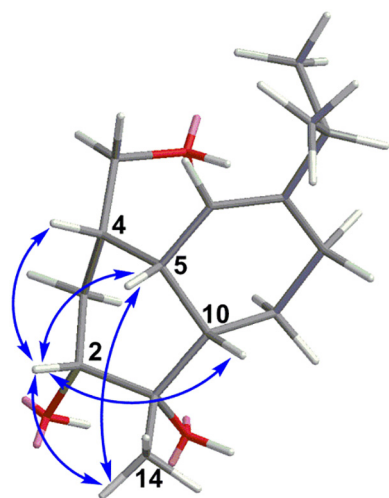


Fig. 3. Key NOESY correlations of compound 7. (For interpretation of the references to colour in this figure legend, the reader is referred to the web version of this article.)

which was determined by comparison with standard sugar via GC. Therefore, compound 6 was determined to be (2,6-dimethoxy-4-hydroxymethyl-phenol) 1-O- β -D-(6-O-*p*-hydroxybenzoyl)-glucopyranoside and was named rhomicranoside F.

Compound 7 was obtained as yellow oil. The molecular formula was confirmed to be $C_{15}H_{26}O_3$. Based on the ^{13}C NMR and DEPT data, 15 carbons were found, including three methyl groups (δ_C 21.8, 22.1, and 23.4), four methylenes (δ_C 25.6, 39.8, 43.8, and 64.3), six methines (δ_C 38.2, 40.5, 42.7, 62.2, 73.9, and 124.6), and two quaternary carbons (δ_C 74.9 and 148.5). These features consist of a (10 \rightarrow 1) abeo-eudesmane sesquiterpene with three oxygenated substituents and a double bond [28,29], which was further confirmed by the HMBC correlations from H₃-14 to C-1 (δ_C 74.9, C), C-10 (δ_C 62.2, CH), and C-9 (δ_C 43.8, CH₂). HMBC correlations from H₃-14, H-5, H-9 and H-10 to C-1 (δ_C 74.9, C), from H-3, H-4 and H-10 to C-2 (δ_C 73.9, CH), and from H-3, H-4 and H-5 to C-15 (δ_C 64.3, CH₂) placed the three hydroxy groups at C-1, C-2, and C-15, respectively. The double bond was determined to be at C-6/7, as suggested by HMBC correlations from H-5, H-8 and H-11 to C-6 (δ_C 124.6, CH) and from H-5, H-9, H-11, H₃-12 and H₃-13 to C-7 (δ_C 148.4, C). The planar structure of 7 was then settled. Moreover, the NOE correlations (Fig. 3) of H-2/H-4, H-2/H-5, H-2/H-10, H-2/H₃-14, and H₃-14/H-5 suggested that these protons were all cofacial (β -oriented). Compound 7 was determined as 1 α ,2 α ,15-trihydroxy-5-*epi*-6-dien-14(10 \rightarrow 1) abeo-eudesmane, and the compound was named rhomicranin I.

Compound 8 was obtained as a white amorphous powder. Its molecular formula was $C_{21}H_{36}O_8$. The NMR spectra showed that 8 was the glycoside of 7. In the HMBC spectrum, the correlations from H-1' to C-15 and from H₂-15 to C-1' indicated that the glycoside was at C-15. The coupling constant of the anomeric proton ($J_{1,2'} = 7.8$ Hz) suggested that glucose was in the β -configuration. The *D*-configuration of the glucose was then determined by GC analyses of the hydrolysate of 8. Thus, compound 8 was tentatively determined as 1 α ,2 α -dihydroxy-5-*epi*-6-dien-14(10 \rightarrow 1) abeo-eudesmane 15-O- β -D-glucoside and was named rhomicranoside G.

The known compounds isolated from the plant are (7*R*,8*S*)-4-hydroxy-9'-O-(α -L-rhamnopyranosyl)-3,3',5'-trimethoxy-8-O-4'-neolignan (9) [22], (2*S*,3*R*)-2,3-dihydro-3-hydroxymethyl-7-methoxy-2-(4'-hydroxy-3'-methoxyphenyl)-5-benzofuranpropanol 3 α -O- α -L-rhamnopyranoside (10) [30], (7*S*,8*R*)-dihydrodehydrodiconiferyl alcohol 9'-O- α -L-rhamnoside (11) [31], 6,7-dihydrocoumarin (12) [32], scopolin (13) [33], ssioriside (14) [34], (-)-secoisolaricinresinol-9-O- β -D-xylopyranoside (15) [35], and (-)-lyoniresinol 3 α -O- β -D-

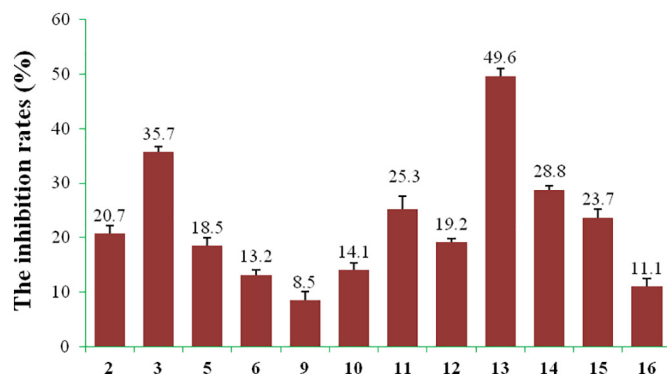


Fig. 4. The inhibitory effects of 2, 3, 5, 6, 9–16 (10 μ M) on the transcription of the NF- κ B-dependent reporter gene in LPS-induced 293T/NF- κ B-luc cells.

xylopyranoside (16) [36]. These structures were identified by comparing their NMR data with data from the published literature.

The isolated compounds were evaluated for anti-inflammatory activities. The inhibitory effects of compounds (2, 3, 5, 6, 9–16) on the NF- κ B signaling pathway are shown in Fig. 4. At a concentration of 10 μ M, several compounds, such as compounds 3, 13, and 14, significantly suppressed the transcription of the NF- κ B-dependent reporter gene in LPS-induced 293T/NF- κ B-luc cells. In addition, these inhibitory effects were not caused by nonspecific cytotoxicity since all tested compounds had no effect on cell viability, as determined by an MTT assay on 293T cells (data not shown). Among the molecules, compound 13, a coumarin glycoside, was more effective than the others (with an inhibition rate of 49.6%).

In conclusion, we demonstrated the isolation and structural determination of 16 compounds from the twigs and leaves of *R. micranthum*. Their structures were determined by extensive spectroscopic analyses. The anti-inflammatory activities of the compounds were evaluated. Among them, compounds 3, 13, and 14 significantly suppressed the transcription of the NF- κ B-dependent reporter gene in LPS-induced 293T/NF- κ B-luc cells. *R. micranthum* is a traditional anti-inflammatory Chinese medicine. However, to date, its anti-inflammatory components are still unclear. These experimental results can not only expand the diversity of chemical structures but also provide evidence for revealing the correlations between chemical constituents and the traditional effects.

Conflict of interest

The authors declare that they have no conflicts of interest.

Acknowledgments

This work was supported by grants from the National Natural Science Foundation of China (Nos. 21572274, 21732008, and 81630094), the CAMS Innovation Fund for Medical Sciences (No. 2016-I2M-3-012), and the Young Elite Scientists Sponsorship Program by CAST (2016QNRC001).

Appendix A. Supplementary data

Supplementary data to this article can be found online at <https://doi.org/10.1016/j.fitote.2019.03.025>.

References

- [1] S.J. Dai, D.Q. Yu, Studies on the flavonoids in stem of *Rhododendron anthopogonoides* II, Chin. J. Chin. Mater. Med. 30 (2005) 1830–1833.
- [2] J.B. Harborne, Flavonoid patterns and phytochemistry: the genus *Rhododendron* section *Vireya*, Phytochemistry 25 (1986) 1641–1643.
- [3] S.J. Jung, D.H. Kim, Y.H. Hong, J.H. Lee, H.N. Song, Y.D. Rho, N.I. Baek, Flavonoids

- from the flower of *Rhododendron yedoense* var. *Poukhanense* and their antioxidant activities, *Arch. Pharm. Res.* 30 (2007) 146–150.
- [4] X. Zhi, L. Xiao, S. Liang, F. Yi, K.F. Ruan, Chemical constituents of *Rhododendron molle*, *Chem. Nat. Compd.* 49 (2013) 454–456.
- [5] Y. Li, Y.B. Liu, J.J. Zhang, Y. Liu, S.G. Ma, J. Qu, H.N. Lv, S.S. Yu, Antinociceptive grayanoids from the roots of *Rhododendron molle*, *J. Nat. Prod.* 78 (2015) 2887–2895.
- [6] Z.R. Zhang, J.D. Zhong, H.M. Li, H.Z. Li, R.T. Li, X.L. Deng, Two new grayanane diterpenoids from the flowers of *Rhododendron molle*, *J. Asian Nat. Prod. Res.* 14 (2012) 764–768.
- [7] S.Z. Chen, S.N. Zhang, L.Q. Wang, G.H. Bao, G.W. Qin, Diterpenoids from the flowers of *Rhododendron molle*, *J. Nat. Prod.* 67 (2014) 1903–1906.
- [8] Y.X. Zhu, Z.X. Zhang, H.M. Yan, D. Lu, H.P. Zhang, L. Li, Y.B. Liu, Y. Li, Antinociceptive diterpenoids from the leaves and twigs of *Rhododendron decorum*, *J. Nat. Prod.* 81 (2018) 1183–1192.
- [9] M.K. Zhang, Y.Y. Xie, G.Q. Zhan, L. Lei, P.H. Shu, Y.L. Chen, Y.B. Xue, Z.W. Luo, Q. Wan, G.M. Yao, Grayanane and leucothane diterpenoids from the leaves of *Rhododendron micranthum*, *Phytochemistry* 117 (2015) 107–115.
- [10] H. Ageta, T. Ageta, Ericaceae constituents: seventeen triterpenoids isolated from the buds of *Rhododendron macrocephalum*, *Chem. Pharm. Bull.* 32 (1984) 369–372.
- [11] D.S. Jun, D.Q. Yu, Triterpenoids of *Rhododendron anthopogonoide* maxim(II), *Chin. J. Nat. Med.* 3 (2005) 347–349.
- [12] Y. Li, Y.X. Zhu, Z.X. Zhang, Y.L. Liu, Y.B. Liu, J. Qu, S.G. Ma, X.J. Wang, S.S. Yu, Diterpenoids from the fruits of *Rhododendron molle*, potent analgesics for acute pain, *Tetrahedron* 74 (2018) 693–699.
- [13] J.F. Zhou, T.T. Liu, H.Q. Zhang, G.J. Zheng, Y. Qiu, M.Y. Deng, C. Zhang, G.M. Yao, Anti-inflammatory grayanane diterpenoids from the leaves of *Rhododendron molle* [J], *J. Nat. Prod.* 81 (2018) 151–161.
- [14] R. Singh, H.S. Rao, Anti-inflammatory activity and effect on gastric acid secretion of Azelain isolated from *Rhododendron dauricum* Linn, *Pharmacogn. Mag.* 4 (2009) 111–114.
- [15] Editorial Committee of Chinese Materia Medica, Chinese Materia Medica (Zhonghua bencao), Shanghai Sci. Technol. Shanghai 7 (1999) 5264–5365.
- [16] L.M. Yang Kuo, L.J. Zhang, H.T. Huang, Z.H. Lin, C.C. Liaw, H.L. Cheng, K.H. Lee, S.L. Morris-natschke, Y.H. Kuo, H.O. Ho, Antioxidant lignans and chromone glycosides from *Eurya japonica*, *J. Nat. Prod.* 76 (2013) 580–587.
- [17] Y.P. Gao, Y.H. Shen, X.K. Xu, J.M. Tian, H.W. Zeng, S. Lin, C.M. Liu, W.D. Zhang, Two novel lignans from *Gaultheria yunnanensis*, *J. Asian Nat. Prod. Res.* 16 (2014) 724–729.
- [18] W. Klyne, R. Stevenson, R.J. Swan, Optical rotatory dispersion. Part XXVIII. The absolute configuration of otobain and derivatives, *J. Chem. Soc. C* (1966) 893–896.
- [19] M. Nishizawa, M. Tsuda, K. Hayashi, Two caffeic acid tetramers having enantiomeric phenyldihydronaphthalene moieties from *Macrotomia euchroma*, *Phytochemistry* 29 (1990) 2645–2649.
- [20] L. Xiong, C.G. Zhu, Y.R. Li, Y. Tian, S. Lin, S.P. Yuan, J.F. Hu, Q. Hou, N.H. Chen, Y.C. Yang, J.G. Shi, Lignans and neolignans from *Sinocalamus affinis* and their absolute configurations, *J. Nat. Prod.* 74 (2011) 1188–1200.
- [21] T. Nakanishi, N. Iida, Y. Inatomi, H. Murata, A. Inada, J. Murata, F. A. Lang, M. Iinuma, T. Tanaka, New neolignan and phenylpropanoid glycosides in *Juniperus communis* var. *Depressa*, *Heterocycles* 63 (2004) 2573–2580.
- [22] X.G. Cheng, J.J. Qin, Q. Zeng, S. Zhang, F. Zhang, S.K. Yan, H.Z. Jin, W.D. Zhang, Taraxasterane-type triterpene and neolignans from *Geum japonicum* Thunb. Var. *chinense* f. *Bolle*, *Planta Med.* 77 (2011) 2061–2065.
- [23] S. Lin, S.J. Wang, M.T. Liu, M.L. Gan, S. Li, Y.C. Yang, Y.H. Wang, W.Y. He, J.G. Shi, Glycosides from the stem bark of *Fraxinus sieboldiana*, *J. Nat. Prod.* 70 (2007) 817–823.
- [24] L. Fang, D. Du, G.Z. Ding, Y.K. Si, S.S. Yu, Y. Liu, W.J. Wang, S.G. Ma, S. Xu, J. Qu, J.M. Wang, Y.X. Liu, Neolignans and glycosides from the stem bark of *Illicium difengpi*, *J. Nat. Prod.* 73 (2010) 818–824.
- [25] C.S. Kim, L. Subedi, S.Y. Kim, S.U. Choi, K.H. Kim, K.R. Lee, Lignan glycosides from the twigs of *Chaenomeles sinensis* and their biological activities, *J. Nat. Prod.* 78 (2015) 1174–1178.
- [26] S.M.O.V. Dyck, G.L.F. Lemière, T.H.M. Jonckers, R. Dommissie, L. Pieters, V. Buss, Kinetic resolution of a dihydrobenzofuran-type neolignan by lipase-catalysed acetylation, *Tetrahedron Asymmetry* 12 (2001) 785–789.
- [27] T. Yuan, C. Wan, A. Gonzálezarrías, V. Kandhi, N.B. Cech, N.P. Seeram, Phenolic glycosides from sugar maple (*Acer saccharum*) bark, *J. Nat. Prod.* 74 (2011) 2472–2476.
- [28] N.N. Yang, Q.Y. Ma, S.Z. Huang, H.F. Dai, Z.K. Guo, X.H. Lu, Y.G. Wang, Z.F. Yu, Y.X. Zhao, Chemical constituents from cultures of the fungus *Marasmiellus ramealis* (bull.) singer, *J. Braz. Chem. Soc.* 26 (2015) 9–13.
- [29] J.E. Dellar, M.D. Cole, A.I. Gray, S. Gibbons, P.G. Waterman, Antimicrobial sesquiterpenes from *Prostanthera* AFF. *melissifolia* and *P. prtundifolia*, *Phytochemistry* 36 (1994) 957–960.
- [30] N. Iida, Y. Inatomi, H. Murata, J. Murata, F.A. Lang, T. Tanaka, T. Nakanishi, A. Inada, New phenylpropanoid glycosides from *Juniperus communis* var. *Depressa*, *Chem. Pharm. Bull.* 58 (2010) 742–746.
- [31] S.K. Sadhu, E. Okuyama, H. Fujimoto, M. Ishibashi, E. Yesilada, Prostaglandin inhibitory and antioxidant components of *Cistus laurifolius*, a Turkish medicinal plant, *J. Ethnopharmacol.* 108 (2006) 371–378.
- [32] F.A. Moharram, M.S. Marzouk, S.M. El-Shenawy, A.H. Gaara, M.E. Kady, Polyphenolic profile and biological activity of *Salvia splendens* leaves, *J. Pharm. Pharmacol.* 64 (2012) 1678–1687.
- [33] M. Kuroyanagi, M. Shiotsu, T. Ebihara, H. Kawai, A. Ueno, S. Fukushima, Chemical studies on *Viburnum awabuki* K. KOCH, *Chem. Pharm. Bull.* 34 (1986) 4012–4017.
- [34] K. Yoshinari, Y. Sashida, H. Shimomura, Two new lignan xylosides from the barks of *Prunus siori* and *Prunus padus*, *Chem. Pharm. Bull.* 37 (1989) 3301–3303.
- [35] Y.H. Wang, Z.K. Zhang, H.P. He, S. Gao, N.C. Kong, M. Ding, X.J. Hao, Lignans and triterpenoids from *Cissus repens* (Vitaceae), *Acta Bot. Yunnanica* 28 (2006) 433–437.
- [36] H. Fuchino, T. Satoh, N. Tanaka, Chemical evaluation of *Betula* species in Japan. I. Constituents of *Betula ermanii*, *Chem. Pharm. Bull.* 43 (1995) 1937–1942.